

DEVELOPMENT OF A BIODEGRADABLE COMPOSITE FILM FROM CHITOSAN, AGAR AND GLYCEROL BASED ON OPTIMIZATION PROCESS BY RESPONSE SURFACE METHODOLOGY

PARTHIBAN FATHIRAJA,* SUGUMAR GOPALRAJAN,** MASILAN KARUNANITHI,**
MURALIDHARAN NAGARAJAN,** MOHAN CHITRADURGA OBAIAH,**
SUKUMAR DURAIRAJ* and NEETHISELVAN NEETHIRAJAN*****

**TNJFU – Fisheries College and Research Institute, Tamil Nadu, India*

***Tamil Nadu Dr. J. Jayalalithaa Fisheries University (TNJFU), Tamil Nadu, India*

****TNJFU – Dr. MGR Fisheries College and Research Institute, Tamil Nadu, India*

*****ICAR – Central Institute of Fisheries Technology, Cochin, Kerala, India*

******TNJFU – Directorate of Incubation and Vocational Training in Fisheries, Tamil Nadu, India*

✉ *Corresponding author: P. Fathiraja, parthiban@tnfu.ac.in*

Received April 15, 2021

The aim of the study has been to develop a biodegradable film from marine polysaccharides. The optimization of polysaccharides quantity for the composite film was sought by empirical response surface methodology. The Box–Behnken Model Design was applied to optimize the concentration of chitosan (1.0-2.0% (w/v), agar (1.0-2.0% (w/v) and glycerol (0.1-0.5% (w/v) as independent variables to achieve the goal. The overall desirability function fits with the quadratic model (0.862043) at a significant level ($p < 0.05$) for the optimum concentration of chitosan (1.5% (w/v), agar (2.0% (w/v) and glycerol (0.41% (w/v) to obtain the minimum water vapor permeability ($7.25 \times 10^{-10} \text{ g m m}^{-2} \text{ Pa}^{-1} \text{ s}^{-1}$) and maximum tensile strength (12.21 Ma P), elongation at break (7.32%) and puncture resistance (16.18 N) in the optimized composite film. The absolute residual errors of experimental and predicted responses were between 1.24 and 3.56% acceptable levels. Attenuated total reflection–Fourier transform infrared spectroscopy confirmed the intermolecular non-covalent hydrogen bond between the hydroxyl groups of agar and glycerol with the amino group of chitosan. 3D atomic force microscopy images revealed that the chitosan, agar and glycerol film has layer-by-layer smooth surface properties due to homogenous interaction among the polysaccharides; this provides the film with good mechanical properties and with functional application. Chitosan was found to be responsible for the lower level of water vapor permeability and higher puncture resistance of the film. Tensile strength and elongation at break were influenced by agar and glycerol. The whiteness of the film was negatively affected with the concentration of chitosan.

Keywords: composite chitosan film, response surface methodology, atomic force microscope, ATR-FTIR, whiteness index

INTRODUCTION

Traditionally, packaging materials are made from poorly biodegradable petroleum derived plastics.^{1,2} The global production of plastics reached 359 million metric tons per year (Mt y^{-1}) for 2018,³ which is very near to the value of global human biomass of around 393 Mt. Moreover, the global scenario of mismanaged plastic waste is projected to reach 155-265 Mt y^{-1} by 2060.⁴ Innovative biopolymer technology is an alternative option for non-degradable plastics and sustainable management of plastic wastes.⁵ Polysaccharides are a class of natural biodegradable polymers that have been getting increasing attention as alternatives for petroleum derived plastics.⁶ Studies have been carried out continuously for the development of biodegradable packaging films using natural polysaccharides sources, such as cereals (corn, rice, oat *etc.*),⁷⁻⁹ tubers (cassava, tapioca, yam, potato *etc.*)¹⁰⁻¹² and marine polysaccharides (chitosan, agar, alginate, carrageenan *etc.*).¹³⁻¹⁶ Marine polysaccharide-based materials have attracted attention as one of the most important research directions in recent years, due to their good biocompatibility, biodegradability, non-toxicity, low cost, and abundance.¹⁷

Chitosan is a natural polymer consisting of (1,4)-linked 2-amino-deoxy-b-D-glucan, a deacetylated derivative of chitin, which is the major constituent of the exoskeleton of crustaceans, and is the second most abundant polysaccharide found in nature after cellulose.¹⁸ Chitosan is non-toxic, biodegradable,

biofunctional, biocompatible, in addition to having antimicrobial characteristics.¹⁹ Moreover, chitosan is an excellent edible film component due to its film-forming capacity and good mechanical properties, it can form transparent films, which can fulfill various packaging needs.²⁰⁻²² However, chitosan films are rigid and need plasticizers and other polysaccharides to reduce its fragility and increase film flexibility. These reduce the intermolecular forces and increase the mobility of polymer chains, thereby improving the flexibility and extensibility of the film and increasing its water vapor and solute permeability.²³

Agar is an unbranched polysaccharide extracted from marine red algae of the class of Rhodophyceae.²⁴ The chemical structure of agar is composed of a mixture of agarpectin (non-gelling fraction) and agarose (gelling fraction).²⁵ Agarpectin is a slightly branched and sulfated polysaccharide, but agarose is a linear polysaccharide, consisting of repetitive units of D-galactose and 3-6 anhydro-L-galactose, linked by alternating α -(1 \rightarrow 3) and β -(1 \rightarrow 4) glycosidic bonds. Agarpectin is removed from agar during commercial production to obtain higher gel strength.^{26,27} One of the most important properties of agar is its ability to form reversible gels, even at low concentration, simply by cooling its hot aqueous solutions. This is due to the formation of hydrogen bonds.²⁸ This has given agar a wide use in a variety of industries, but blending agar with other polymers to make biodegradable films is very uncommon. Film prepared from plain agar and chitosan are not considered of much importance because of their brittleness, high WVP, and poor thermal stability.²⁴ Researches have been carried out to improve polymer interactions and networks by blending different biological polysaccharides and gums to produce composite films with improved physico-chemical and mechanical properties, such as tensile strength (TS), elongation at break (EB) and puncture resistance (PR).²⁹⁻³⁶

Seaweed polysaccharides consist of numerous monosaccharides linked by glycosidic bonds and broadly grouped into sulfated and non-sulfated polysaccharides. The network and structural interaction among the groups offer interesting functional properties.³⁷ The gels can be rigid, flowing, brittle, sparingly firm, soft, spreadable, sliceable, rubbery, or grainy, depending upon the degree of interaction between the polymers and their ratio.³⁸ Agar interacting with other saccharides enhances the physico-chemical properties by hysteresis, which makes agar a functional ingredient.³⁹ It can also control syneresis in gel networks, due to the non-digestible nature of agar.⁴⁰ Studies have been carried out on prospects of developing polysaccharide-based composite films; among them, polysaccharide-based materials from seaweeds promise to expand the future applications of biodegradable films.⁴¹⁻⁴³

Plasticizers are used to improve physical and mechanical properties of films, when added to the film forming solutions before casting, by decreasing their stiffness. They also help maintain film properties during longer storage periods.⁴⁴ Plasticizers reduce film fragility by decreasing the hydrogen bonds between the polymer chains and increasing the intermolecular space to improve flexibility and reduce cohesion.⁴⁵ Mostly, polyols (glycerol, sorbitol and polyethylene glycol), sugars (glucose and honey) and fats (monoglycerides, phospholipids and surfactants) are used as plasticizers in packaging film formation.⁴⁶ Glycerol is the most widely used plasticizer for improving the properties of edible films.⁴⁷ Since marine polysaccharides are sensitive to moisture and have low mechanical strength, additional research is necessary to improve their properties and reduce the cost of the final product.^{48,49} The present work focuses on the development and application of polysaccharides as multifunctional materials in the food packaging sector.

Since chitosan and agar are known for their film-forming ability, due to the presence of hydrogen bonding in their structure, while glycerol influences bonding, blending these ingredients is expected to help obtain films with improved mechanical properties. The antibacterial properties of chitosan would also contribute to extending the shelf life of food products, when it is used as packaging material. In this study, we report on the optimization of the composition of film blends prepared from chitosan, agar and glycerol (CAG) to enhance the physico-chemical, mechanical and optical properties of the obtained films.

Response surface methodology–Box-Behnken design (RSM–BBD) is a widely accepted statistical technique for experimental design, model building and optimization of process conditions.⁵⁰ Previous studies have used RSM to optimize the physico-chemical and mechanical parameters of films, especially, of composite films, such as chitosan-gelatin-based hybrid polymer network,⁵¹ alginate-glycerol-citric acid.⁵² A blend of chitosan, agar and glycerol (CAG) has not been investigated so far and therefore, this study aimed to use this tool for optimizing the process variables in the development

of a biodegradable film based on chitosan, agar and glycerol, with desirable properties of minimum WVP and maximum TS, PR and EB.

EXPERIMENTAL

Materials and chemicals

Commercial grade chitosan (molecular weight of 75.6 kDa, 92% degree of deacetylation and 100 cps viscosity) was obtained from ISF Chitin & Marine Products LLP, Cochin, Kerala, India. Purified agar powder (molecular weight of 336.33) was purchased from Himedia, Mumbai, India. All analytical grade chemicals and the solvent were procured from Sigma-Aldrich (Gottingen, Germany). Miscellaneous analytical grade chemicals, such as silica gel, sodium hydroxide, and food grade glycerol were purchased from Rankem (Mumbai, India).

Experimental design

RSM was performed with Design Expert-® 12 (Stat Ease, Minneapolis, USA) based on Box–Behnken experimental design (BBD). The factorial portion, as shown in Table 1, was a full factorial design, with all combinations of the factors at three levels (+1 high, 0 center point, and -1 low). A total of 17 sample runs were performed for analysis, which included 5 central points and 12 true and axial points to estimate repeatability (Table 2). Different concentrations of chitosan from 1 to 2% (A, % w/v), agar from 1 to 2% (B, % w/v) and glycerol from 0.1 to 0.5% (C, % w/v) were chosen as independent variables. All experimental runs were performed in three replications and the mean values of mechanical properties were used for BBD-RSM. The suggested ANOVA-Quadratic model was used to evaluate the responses for WVP, TS, EP and PR based on the interactions of film components through fit statistics at a 5% level of significance. BBD was used for data analysis and graphing (contour and 3D plot) outputs. The numerical optimization function was performed by the desirability plot, targeting minimum WVP and maximum TS, EP and PR. The finalized experimental film developed was based on the calculated factor values from the point of prediction. The response data of the optimized film were confirmed by predicted responses by absolute % error. All data were presented as mean \pm standard deviation and the probability value of $P < 0.05$ was considered significant using the statistical package for social sciences (IBM-SPSS 22.0 for Windows, SPSS Inc., Chicago, USA)

Film preparation

The CAG composite film was prepared with a slight modification of the method described by Blanco-Pascual *et al.*⁵³ The composite film solution (CFS) was prepared by dissolving the polysaccharides and glycerol as per the run value obtained from BBD-RSM. The required quantity of chitosan was dissolved in 1% acetic acid by continuous agitation at 600 rpm for two days in a magnetic stirrer (Remi, Mumbai, India). The mixture was strained through a muslin filter cloth to remove impurities. The agar and glycerol were suspended separately in the chitosan solution and then mixed together with the help of magnetic stirrers at 600 rpm for 20 min under controlled conditions to obtain a homogenous CAG mixture. The complete solubilization of the CAG mixture was carried out in a hot water bath at 95 °C, 45 min with continuous agitation. The solubilized CFS mixtures were casted at the temperature of 80 °C on silicon trays arranged in a cabinet drier at a level of 0.5 mL/cm². The trays were dried at 45 °C for 24 h in the cabinet drier after gel setting. The films were peeled off and stored in a desiccator for conditioning at 25 °C, 50% RH for 48 h. These prepared films were evaluated in terms of their physico-chemical, mechanical and optical properties.

Table 1
Level of independent variables

Independent variables	Codified independent variables	Levels of coded variables		
		-1	0	+1
Chitosan (%)	A	1	1.5	2
Agar (%)	B	1	1.5	2
Glycerol (%)	C	0.1	0.3	0.5

A – codified chitosan independent variable, B – codified agar independent variable, C – codified glycerol independent variable; Coded variables levels (factor -1 is a low level, factor 0 is the center point and factor +1 is a high level)

Table 2
Box-Behnken experimental design response variables

Run	Independent variables			Observed value of response variables			
	A	B	C	WVP	TS	EB	PR
1	1	-1	0	3.76±0.16 ^c	8.75±0.69 ^a	4.47±0.17 ^a	17.31±2.17 ^{cd}
2	-1	0	1	28.43±0.11 ^l	11.21±1.49 ^{cd}	6.98±0.67 ^{defg}	15.53±2.12 ^{abcd}
3	-1	0	-1	21.76±0.17 ^j	10.46±1.69 ^{bcd}	6.22±0.46 ^{cefg}	11.74±2.55 ^a
4	1	1	0	0.56±0.12 ^a	9.81±0.67 ^{abc}	5.78±0.8 ^{bcd}	17.1±1.99 ^{cd}
5	0	0	0	5.47±0.18 ^d	11.23±0.14 ^{cd}	6.83±0.38 ^{defg}	14.33±1.77 ^{abcd}
6	1	0	1	0.86±0.08 ^a	9.23±0.99 ^{ab}	5.64±0.62 ^{bc}	17.67±1.64 ^d
7	0	0	0	5.82±0.09 ^d	11.32±1.6 ^{cd}	6.82±0.83 ^{defg}	14.32±1.77 ^{abd}
8	-1	-1	0	25.56±0.07 ^k	9.87±0.85 ^{abc}	5.87±0.32 ^{bcd}	12.37±1.88 ^{abc}
9	0	0	0	5.74±0.11 ^d	11.34±0.82 ^{cd}	6.82±0.54 ^{defg}	14.32±2.49 ^{abcd}
10	0	0	0	5.61±0.11 ^d	11.26±0.54 ^{cd}	6.83±0.52 ^{defg}	14.33±2.22 ^{abc}
11	-1	1	0	20.74±0.15 ⁱ	11.98±0.73 ^d	7.02±1.16 ^{fg}	15.73±1.88 ^{bcd}
12	0	-1	-1	12.45±0.19 ^g	9.21±0.44 ^{ab}	5.24±0.48 ^{abc}	13.32±1.77 ^{abc}
13	0	0	0	5.37±0.16 ^d	11.3±0.33 ^{cd}	6.81±0.38 ^{defg}	14.31±1.53 ^{abcd}
14	1	0	-1	3.27±0.21 ^b	9.12±0.6 ^{ab}	4.82±0.83 ^{ab}	15.9±1.55 ^{bcd}
15	0	1	-1	10.47±0.5 ^f	11.34±0.36 ^{cd}	6.38±0.56 ^{cefg}	15.38±1.88 ^{abcd}
16	0	1	1	9.78±0.75 ^e	11.74±0.81 ^d	7.21±0.67 ^g	16.71±2.08 ^{cd}
17	0	-1	1	16.74±0.3 ^h	10.24±0.6 ^{abcd}	6.38±0.61 ^{cefg}	16.48±2.89 ^{cd}

A – codified chitosan independent variable, B – codified agar independent variable, C – codified glycerol independent variable; WVP – water vapor permeability ($10^{-10} \text{ g m m}^{-2} \text{ Pa}^{-1} \text{ s}^{-1}$), TS – tensile strength (MPa), EB – elongation at break (%) and PR – puncture resistance (N); Different letters in the same column indicate significant differences ($p < 0.05$), Mean \pm SD ($n = 3$)

Physico-chemical properties

Moisture content (MC)

The MC of the CAG composite film was estimated by the gravimetric method.⁵⁴ The initial and final masses of rectangular samples ($\sim 2 \text{ cm}^2$) were noted on an analytical balance (Shimadzu Corporation, Kyoto, Japan). The oven temperature was set to $105 \pm 1 \text{ }^\circ\text{C}$ for 24 h for drying the film. The results were expressed as the percentage of moisture content using the following equation:

$$\text{MC \%} = (\text{M1} - \text{M2}) \text{M1}^{-1} \times 100 \quad (1)$$

where M1 – initial mass, M2 – dry mass.

Film thickness

A precise digital micrometer with ± 0.001 accuracy (Safeseed Micrometer Screw Gauge, Chennai, India) was used to determine the thickness of the films. Measurements were performed randomly at ten different locations of the samples.⁵⁵ The average value of film thickness was used to calculate physico-chemical and mechanical properties.

Whiteness index (WI)

The WI of the CAG composite film was measured using a Hunter Lab Scan XE Spectrocolorimeter (Hunter Associates Laboratory, Reston, VA, USA), with a D-65 illuminant and observer angle of 10° . The values of lightness (L^*), redness (a^*), and yellowness (b^*) of the films were measured after calibration of the instrument against a standard white screen. Films with the size of 25 cm^2 were placed on the plate of the instrument and then color quantity indices L^* , a^* and b^* were observed for the calculation of the whiteness index with the following equation:⁵⁶

$$\text{WI} = 100 - [(100 - L^*)^2 + (a^*)^2 + (b^*)^2]^{1/2} \quad (2)$$

where ΔL^* , Δa^* and Δb^* are difference in corresponding color parameters between the CAG composite film and the white standard.

Film transparency

The transparency of the films was assessed according to procedure described by Han and Floros.⁵⁷ The pre-conditioned film strips were fixed onto a cuvette and then absorbance at 600 nm was measured using a UV-visible spectrophotometer (UNICO Model SQ2800, Suite E Dayton, NJ 08810 USA). The film transparency was calculated with the following formula:

$$\text{T\%} = A_{600} I^{-1} \quad (3)$$

where T is transparency, A_{600} – absorbance at 600 nm and l^{-1} – film thickness in mm. Higher transparency values represent less transparent films.

Film swelling (FS) and film erosion (FE)

All experimental films were dried in vacuum at room temperature for 24 h and the sample piece ($1 \times 1 \text{ cm}^2$) was accurately weighed. After initial weighing, they were kept in a beaker with 50 mL of distilled water at $37 \pm 0.5 \text{ }^\circ\text{C}$ for 1 h, then the films were wiped to remove moisture and wet mass was reweighed. The swollen films were oven-dried at $60 \text{ }^\circ\text{C}$ (Technico, Chennai, India) for 24 h to calculate percentage erosion after dried weights were taken. The percentage weight gain and percentage weight loss were expressed as film swelling and erosion using the equations:⁵⁸

$$\text{FS\%} = (M_{\text{swelling}} - M_{\text{initial}})(M_{\text{initial}})^{-1} \times 100 \quad (4)$$

$$\text{FE\%} = [M_{\text{initial}} - M_{\text{final}}](M_{\text{initial}})^{-1} \times 100 \quad (5)$$

where M is mass.

Water vapor permeability (WVP)

The ASTM E96/E96M modified gravimetric cup method was followed to determine the WVP of the CAG composite films.⁵⁹ Water vapor permeability of the films was measured by keeping the sample films tightly adhering to the top of glass vials (35 cm^3). Each sample vial was filled with pre-weighed anhydrous calcium chloride, and a control vial of glass of identical weight with the sample vials was also used. Then, the experimental vials were kept in a desiccator maintaining $90 \pm 5\%$ RH with a saturated sodium chloride solution at $30 \pm 2 \text{ }^\circ\text{C}$. The mass gain was measured after a 2 h interval. The changes in the average mass of the vials (in triplicate) were used to calculate the WVP using the equation:

$$\text{WVP} (\text{g m}^{-2} \text{ Pa}^{-1} \text{ s}^{-1}) = W l A^{-1} t^{-1} \Delta P^{-1} \quad (6)$$

where W is the weight gain of the vial (g), l is the film thickness (m), A is the exposed area of the film (m^2), t is the time of gain (s), and ΔP is the vapor pressure difference (Pa).

Mechanical properties

The tests were carried out according to the ASTM D-882 standard test.⁶⁰ Tensile strength (TS), elongation at break (EB) and puncture resistance (PR) of the CAG composite films were evaluated for 17 sample runs as per BBD-RSM, using a Universal Testing Machine (Lloyd Instruments, Hampshire, UK).⁶¹ The test was performed at $25 \text{ }^\circ\text{C}$ and $50 \pm 5\%$ RH controlled condition. Film samples of $8 \times 1.5 \text{ cm}^2$, clamped with the additional grip length of 3 cm on both sides, were used for testing. The film samples were deformed under a 100 N load cell, with the cross-head speed of 50 mm/min, to break them at the center point. The initial slope of the stress–strain curve, maximum load and final extension at break were used to calculate TS, EB and PR, respectively, as follows:

$$\text{TS} (\text{M Pa}) = \text{Maximum load (kg)} (\text{Cross-section area (mm}^2))^{-1} \quad (7)$$

$$\text{EB} (\%) = (\text{Change in length at break after stretching}) (\text{Original length})^{-1} \times 100 \quad (8)$$

$$\text{PR} (\text{N}) = \text{Load required to puncture film} \quad (9)$$

Attenuated total reflection – Fourier transform infrared spectroscopy (ATR-FTIR)

High quality ATR-FTIR spectra of the CAG composite film were recorded by a Nicolet iS5 FTIR spectrometer, equipped with an ATR/ID3 with an argon horizontal cell (Thermo Fisher Scientific, Waltham, Massachusetts, USA) with controlled atmosphere. The spectra in the range of $4,000\text{--}400 \text{ cm}^{-1}$ were recorded with 32 scans at a resolution of 4 cm^{-1} . The scanning was performed to gain automatic signals recorded against a background spectrum in the clean empty cell at $16 \text{ }^\circ\text{C}$.⁶² The peaks of transmittance at different wavenumbers of the optimized CAG composite film were compared with those obtained for individually developed films from chitosan and agar with glycerol as plasticizer.

Atomic force microscopy (AFM) analysis

Atomic force microscopy (AFM) images were recorded on a Nanosurf Easy Scan 2 AFM (Graubernstrasse 12, 4410 Liestal, Switzerland) instrument to obtain topographical images of the films.⁶³ It provides 3D visualization and both qualitative and quantitative information on many physico-chemical properties, including size, morphology, surface texture and roughness. A range of 1 nanometer to 8 micrometers particle sizes can be characterized in the same scan. The sample was visualized in the non-contact mode with a 10 nm diameter tip. The CAG composite film image was generated at 300×300 pixels resolution.

RESULTS AND DISCUSSION

Physico-chemical properties

Moisture content (MC)

The MC greatly influences the physico-chemical and mechanical properties of biodegradable films, which play a vital role in food packaging applications.⁶⁴ The range of MC for the 17 experimental runs was noticed to be from $9.18 \pm 0.76\%$ to $14.93 \pm 0.72\%$ (Table 3). These results were slightly lower than those for an edible film prepared from chitosan and a green tea extract composite film ($14.19 \pm 1.6\%$ to 19.09 ± 1.7),⁶⁵ as well as those of glutinous rice starch chitosan composite films ($14.11 \pm 0.99\%$ to $17.04 \pm 2.23\%$).⁶⁶ The concentration of glycerol directly influences the moisture retention due to the water holding capacity as a reflection of hydrogen bonding.⁶⁷ Other reports also showed a positive correlation of the level of glycerol and MC in chitosan based films.^{68,69} The moderate level of MC obtained in the CAG composite films describes the water insoluble characteristics of chitosan rather than agar.

Film thickness

The thickness of the CAG composite films varied ($p < 0.05$) in this study, ranging from 83.12 ± 1.89 to $121 \pm 2.9 \mu\text{m}$ (Table 3). The thickness of the films has a role in mechanical properties, such as TS, EB and WVP,⁷⁰ and highly depends on composition and processing parameters.⁷¹ The thickness increases with a higher level of glycerol, because the glycerol molecules occupy the voids in the matrix and interact with the film forming polymer.⁷² Comparable results have been reported for a chitosan and gelatin film, ranging from 75.0 ± 20 to $106 \pm 11 \mu\text{m}$,¹ and for a film developed from pea starch and chitosan, ranging from 67.7 to 124.6 μm .⁷³

Whiteness index (WI)

The observed a^* values from 1.43 to 11.64 for the CAG composite film indicate less light green to red color, and b^* values of 1.15 to 11.95 denote yellowness. The WI (ΔE) value of the CAG composite film is presented in Table 3. It was noticed that ΔE values ranged from 12.78 ± 0.45 to 38.67 ± 1.47 for the 17 samples in the experimental design. Similar ranges of results were reported for a film prepared from alginate with incorporated essential oil extracted from medicinal plants.⁷⁴ The higher level of L^* values of the films always express the whiteness of the sample, which is preferred for a packaging film material. The brightness value of the CAG composite was comparatively lower than the brightness of the previously reported gelatin film developed from tilapia skin (1.87 to 2.51), which can be explained by the varying nature of the source.⁷⁵

Table 3
Observed values for non-optimized response variables

Run	MC	L	WI	T	S	E
1	$13.18 \pm 0.56^{\text{fg}}$	$96 \pm 1.67^{\text{ef}}$	$19.47 \pm 1.43^{\text{c}}$	$1.94 \pm 0.28^{\text{abc}}$	$62.57 \pm 0.47^{\text{g}}$	$2.6 \pm 0.32^{\text{ab}}$
2	$13.87 \pm 0.47^{\text{gh}}$	$92 \pm 1.87^{\text{cd}}$	$32.47 \pm 1.26^{\text{f}}$	$1.64 \pm 0.14^{\text{a}}$	$64.38 \pm 0.53^{\text{h}}$	$4.2 \pm 0.12^{\text{c}}$
3	$9.18 \pm 0.76^{\text{b}}$	$87 \pm 1.67^{\text{b}}$	$34.54 \pm 1.46^{\text{f}}$	$1.53 \pm 0.15^{\text{a}}$	$53.42 \pm 0.38^{\text{b}}$	$2.7 \pm 0.35^{\text{ab}}$
4	$13.93 \pm 0.52^{\text{gh}}$	$121 \pm 2.09^{\text{j}}$	$12.78 \pm 0.45^{\text{a}}$	$2.32 \pm 0.09^{\text{c}}$	$66.45 \pm 0.73^{\text{j}}$	$2.7 \pm 0.43^{\text{ab}}$
5	$11.43 \pm 0.76^{\text{de}}$	$95 \pm 1.76^{\text{de}}$	$18.49 \pm 1.67^{\text{bc}}$	$1.97 \pm 0.22^{\text{abc}}$	$57.32 \pm 0.25^{\text{d}}$	$2.8 \pm 0.52^{\text{ab}}$
6	$13.92 \pm 0.43^{\text{gh}}$	$105 \pm 1.46^{\text{i}}$	$13.45 \pm 1.72^{\text{a}}$	$2.28 \pm 0.41^{\text{c}}$	$65.38 \pm 0.12^{\text{i}}$	$3.4 \pm 0.68^{\text{ab}}$
7	$11.48 \pm 0.76^{\text{de}}$	$97 \pm 1.98^{\text{ef}}$	$18.34 \pm 0.95^{\text{bc}}$	$1.94 \pm 0.32^{\text{abc}}$	$57.64 \pm 0.8^{\text{d}}$	$2.7 \pm 0.62^{\text{abc}}$
8	$10.13 \pm 0.32^{\text{bc}}$	$84 \pm 1.09^{\text{ab}}$	$38.67 \pm 1.47^{\text{g}}$	$1.47 \pm 0.15^{\text{a}}$	$55.68 \pm 0.67^{\text{c}}$	$2.6 \pm 1.41^{\text{ab}}$
9	$11.47 \pm 0.84^{\text{de}}$	$95 \pm 1.78^{\text{de}}$	$18.39 \pm 1.42^{\text{bc}}$	$1.92 \pm 0.39^{\text{abc}}$	$58.92 \pm 0.38^{\text{e}}$	$2.8 \pm 0.15^{\text{ab}}$
10	$11.52 \pm 0.68^{\text{de}}$	$96 \pm 1.96^{\text{ef}}$	$18.58 \pm 1.67^{\text{bc}}$	$1.89 \pm 0.18^{\text{abc}}$	$59.14 \pm 0.82^{\text{e}}$	$2.9 \pm 0.36^{\text{ab}}$
11	$13.47 \pm 0.48^{\text{g}}$	$97 \pm 1.76^{\text{ef}}$	$29.56 \pm 1.87^{\text{e}}$	$1.76 \pm 0.07^{\text{ab}}$	$64.34 \pm 0.92^{\text{h}}$	$3.2 \pm 0.32^{\text{ab}}$
12	$7.87 \pm 0.67^{\text{a}}$	$83 \pm 1.89^{\text{a}}$	$25.93 \pm 2.04^{\text{d}}$	$1.89 \pm 0.15^{\text{abc}}$	$51.76 \pm 0.47^{\text{a}}$	$3 \pm 0.82^{\text{abc}}$
13	$11.45 \pm 0.82^{\text{de}}$	$95 \pm 1.45^{\text{de}}$	$18.68 \pm 2.34^{\text{bc}}$	$1.88 \pm 0.15^{\text{abc}}$	$58.78 \pm 0.54^{\text{c}}$	$2.7 \pm 0.74^{\text{ab}}$
14	$9.28 \pm 0.18^{\text{b}}$	$101 \pm 2.9^{\text{gh}}$	$14.53 \pm 1.78^{\text{a}}$	$2.23 \pm 0.26^{\text{bc}}$	$54.28 \pm 0.62^{\text{b}}$	$2.3 \pm 0.56^{\text{a}}$
15	$10.45 \pm 0.73^{\text{cd}}$	$99 \pm 1.27^{\text{fg}}$	$17.64 \pm 2.13^{\text{bc}}$	$1.96 \pm 0.36^{\text{abc}}$	$56.76 \pm 0.92^{\text{d}}$	$2.5 \pm 0.67^{\text{a}}$
16	$14.93 \pm 0.72^{\text{h}}$	$104 \pm 1.78^{\text{hi}}$	$15.76 \pm 1.34^{\text{ab}}$	$2.16 \pm 0.17^{\text{bc}}$	$78.47 \pm 0.28^{\text{k}}$	$3.8 \pm 0.39^{\text{bc}}$
17	$12.25 \pm 0.72^{\text{ef}}$	$91 \pm 1.68^{\text{c}}$	$27.36 \pm 2.18^{\text{de}}$	$1.82 \pm 0.45^{\text{abc}}$	$61.47 \pm 0.14^{\text{f}}$	$3.2 \pm 0.69^{\text{abc}}$

MC – moisture content (%), L – thickness (μm), WI – whiteness index, T – transparency, S – swelling (%), E – erosion (%); Different letters in the same column indicate significant differences ($p < 0.05$) Mean \pm SD ($n = 3$)

Film transparency

The transparency of films is an auxiliary criterion to judge the compatibility of the components.⁷⁶ The CAG composite film had transparency values of 1.53 ± 0.15 to $2.28 \pm 0.41\%$ (Table 3), the lower transparency values represent more transparent characteristics of the film. The transparency of the CAG composite film is lower than that of a reported orange peel powder and gelatin composite film (0.53 ± 0.06 to $1.28 \pm 0.04\%$),⁷⁷ and comparable with that of a chitosan-gelatin film (0.67 ± 0.01 to 5.00 ± 0.02).¹ Higher transparency of the film gives an indication of complete solubilization of the polysaccharides and of uniformity in the three-dimensional network of the film. The overall transparency of a packaging material enhances its attractiveness and influences consumer acceptability of the products.⁷⁸

Film swelling and film erosion

The swelling phenomenon in hydrogels has been attributed to the hydrophilic functional groups, such as COO^- and NH_2^- of the biopolymers. The erosion is endorsed by a loosely bound network among biopolymers and strong affinity with external water molecules.⁷⁹ The swelling ratio for the samples in the experimental design was less than 100% (51.76 ± 0.47 to $78.47 \pm 0.28\%$ (Table 3)). The swelling behavior of the developed film was lesser than that observed previously for a chitosan, oxidized pectin and polyvinyl alcohol film (362.12 to 1634.25%) at different concentration levels. The hydrophilic groups of agar might have aligned with chitosan into three dimensional networks. Polymer erosion in the film microstructure changes with the degree of polymerization.⁸⁰ The film erosion indicates reduction of the mass from the network matrices due to the water diffusion.⁸¹ The study results showed an erosion range from $2.3 \pm 0.56\%$ to $4.2 \pm 0.12\%$, which supported the insoluble nature of chitosan in polar compounds. The CAG films had a lower erosion rate than that of a rice starch and chitosan composite film.⁶⁶ The CAG composite films had better swelling and erosion properties than those of the reference chitosan based films.

Water vapor permeability (WVP)

WVP is one of the most important physico-chemical properties of food packaging materials, which governs the ability of a food package to control moisture transfer from the atmosphere to the food or *vice versa*.⁸² Polysaccharide-based films are subjected to more water vapor transmission due to their hydrophilic nature.²⁷ Therefore, the experimental design with 17 runs with combinations of the variables revealed a range from $0.56 \pm 0.12 \times 10^{-10} \text{ g m/Pa s m}^2$ to $28.43 \pm 0.11 \times 10^{-10} \text{ g m/Pa s m}^2$ (Table 2). These values were lesser than the range obtained for pea starch and chitosan composite films ($4.16 \times 10^{-10} \text{ g m/Pa s m}^2$ to $34.4 \times 10^{-10} \text{ g m/Pa s m}^2$)⁷³ and comparable with those for the pearl millet, carrageenan and glycerol composite films ($0.65 \times 10^{-10} \text{ g m/Pa s m}^2$ to $3.31 \times 10^{-10} \text{ g m/Pa s m}^2$).⁸³

The experimental data fit the quadratic mathematical model, which implies the following relationship between independent variables: $\text{WVP} = + 5.60 - 11.00 \text{ A} - 2.12 \text{ B} + 0.9825 \text{ C} + 0.4050 \text{ AB} - 2.27 \text{ AC} - 1.25 \text{ BC} + 4.14 \text{ A}^2 + 2.92 \text{ B}^2 + 3.84 \text{ C}^2$. The ANOVA summary implied that the model was significant (Table 4), as the proposed equation matched 99.56%. The Predicted R^2 of 0.9707 is in reasonable agreement with the Adjusted R^2 of 0.9956; *i.e.* the difference is much less than 0.2. The Lack of Fit F-value of 21.67 implies the Lack of Fit is significant as per the experimental values.

The effect of all three independent variables on WVP can be seen in Figure 1 (a, b and c). The agar and glycerol have less influence in controlling WVP than chitosan. Agar has minimal control over WVP, along with glycerol (Fig. 1c), while chitosan has been found to control WVP better than glycerol (Fig. 1b). The combination of agar and chitosan leads to a very good control over WVP (Fig. 1a), which could be due to the network developed by the functional groups of chitosan and agar. Lower WVP of the composite films might be attributed to an increased crosslinking effect, which leads to increased chain to chain interactions in polymers, thereby resulting in stronger films with less permeability to water and gases.⁸⁴ Similarly, the WVP rate could be reduced by an increase in the chitosan levels due to the presence of intense hydrogen bonding between the NH_2 and OH groups of chitosan and agar, respectively, and the results of earlier reports highly correlate with the present study.^{73,85} The unchanged level of WVP values of the film upon an increase in the concentration of agar and glycerol is due to the diffusion of water molecules from the film network. The bonds developed by agar and glycerol might be similar to those in a starch and glycerol film.⁸⁵ The WVP of

packaging films are attributed to several reasons, such as mobility of polymer chains, functional group interaction, integrity of the film, hydrophilic and hydrophobic components ratio *etc.*^{86,87}

Mechanical properties

Tensile strength (TS)

TS is an important mechanical property to explore for any kind of films proposed for food packaging, as it represents the resistance to break at elevated loads or film deformation. The level of TS always influences the application of specific packaging materials to the right products.⁸⁸ TS should be high enough to give mechanical integrity to the content, so that the food gets protected from the wear and tear during transportation and storage.⁶⁶ The data collected for the experimental CAG films revealed the range from 8.75 ± 0.69 to 11.98 ± 0.73 MPa (Table 2). The analysis of experimental data suits the quadratic mathematical model implied in the data. It gave a relationship between independent variables as shown in the equation: $TS = + 11.29 - 0.8263 A + 0.8500B + 0.2863C - 0.2625 AB - 0.1600 AC - 0.1575 BC - 0.9075 A^2 - 0.2800 B^2 - 0.3775C^2$. The ANOVA implied the model was significant (Table 4), where the proposed equation matched 99.00%. The Predicted R² of 0.9368 is in reasonable agreement with the Adjusted R² of 0.9900; *i.e.* the difference is less than 0.2. The Lack of Fit F-value of 11.20 implies it is significant as per the experimental values. There is only a 0.24% chance that a Lack of Fit F-value this large could be caused by noise.

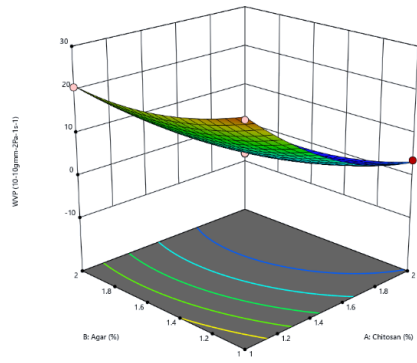
TS is influenced by the presence of agar, which plays a vital role in the experimental films, followed by glycerol (Fig. 2 a, b, c). The influence of agar on TS was found to be higher (Fig. 2a) than that of chitosan (Fig. 2b). The effect of agar and glycerol was highly positive on TS (Fig. 2c), while the effect of chitosan was negative (Fig. 2 a, b). The increasing effect of agar on TS has also been reported for agar based edible films,⁸⁹ thus supporting the research findings. The TS values of the experimental samples were also comparable with those of other biodegradable packaging films with incorporated plant extracts,⁸⁹ however the values are lower than those of petroleum based film materials.⁹⁰

Elongation at break (EB)

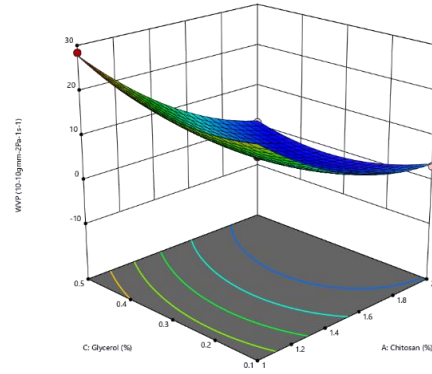
EB is another important mechanical property of biopolymer films, it is the measure of the stretchable/extensible capacity before breaking. The EB values of the CAG films ranged between $4.47 \pm 0.17\%$ and $7.21 \pm 0.67\%$ (Table 2), and these values were comparable with those for rice starch chitosan composite films⁶⁶ and plant extract based composite films.⁹¹ The EB values of CAG are higher than those of polystyrene (PS; 1%-4%) and lower than those of polyamide (PA; 5%-10%), low-density polyethylene (LDPE; 200%-900%), polyvinyl alcohol (PVA; 220%-250%) and polyvinyl alcohol-co-ethylene (EVOH; 180%-250%). The ANOVA implied the model was significant (Table 4), which could describe at least 98.92% of the total variations, and revealed a quadratic relationship between EB and other independent variables ($EB = + 6.82 - 0.6725 A + 0.5538 B + 0.4438 C + 0.0400 AB + 0.0150 AC - 0.0775 BC - 0.7123 A^2 - 0.3248 B^2 - 0.1947 C^2$).

Table 4
ANOVA summary statistics

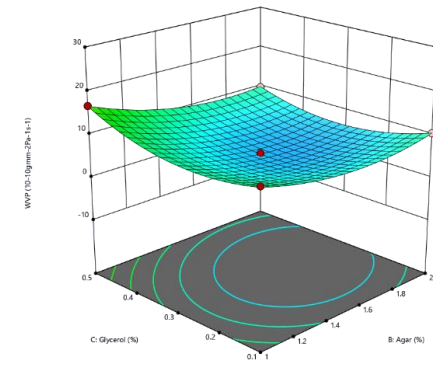
Response	Source	SS	df	MS	F-value	p-value	R ²	Radj	Remark
WVP	Model	189.42	3	63.14	185.79	< 0.0001	0.9956	0.9707	Quadratic
WVP	Lack of fit	2.24	3	0.7470	21.67	0.0062			
TS	Model	4.75	3	1.58	147.56	< 0.0001	0.9900	0.9368	Quadratic
TS	Lack of fit	0.0672	3	0.0224	11.20	0.0205			
EB	Model	2.96	3	0.9866	136.61	< 0.0001	0.9892	0.9247	Quadratic
EB	Lack of fit	0.0503	3	0.0168	239.40	< 0.0001			
PR	Model	4.74	3	1.58	46.91	< 0.0001	0.9883	0.9184	Quadratic
PR	Lack of fit	0.2356	3	0.0785	1121.79	< 0.0001			



(a)

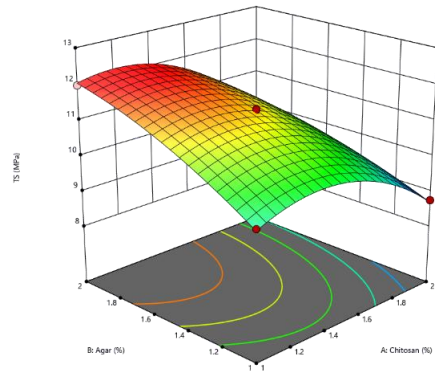


(b)

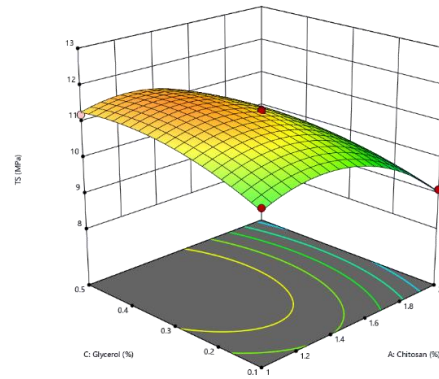


(c)

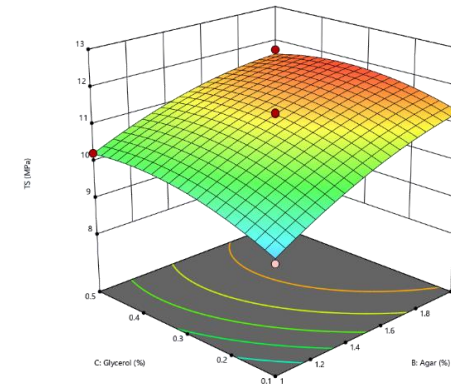
Figure 1: Response surface graphs: (a) Effect of chitosan and agar on water vapor permeability, (b) Effect of chitosan and glycerol on water vapor permeability (c) Effect of agar and glycerol on water vapor permeability



(a)



(b)



(c)

Figure 2: Response surface graphs: (a) Effect of chitosan and agar on tensile strength, (b) Effect of chitosan and glycerol on tensile strength, (c) Effect of agar and glycerol on tensile strength

The Predicted R^2 of 0.9247 is in reasonable agreement with the Adjusted R^2 of 0.9892; with a difference of less than 0.2. The Lack of Fit F-value of 239.40 implied it is significant as per the experimental values and there is only a 0.01% chance of a Lack of Fit. All three independent variables analyzed have a significant ($p < 0.05$) influence on EB in quadratic terms.

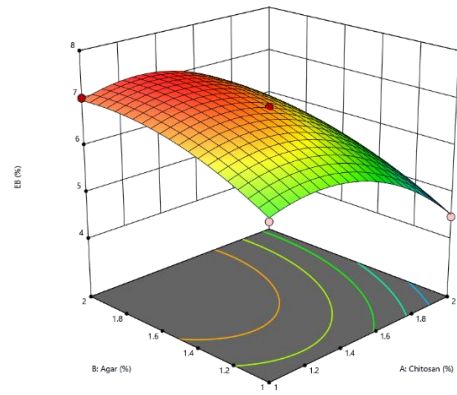
EB is mostly influenced by the presence of agar in the experimental CAG films, followed by glycerol (Fig. 3 a, b, c). EB was also influenced more by agar (Fig. 3a) than by chitosan (Fig. 3b). Agar and glycerol had a highly positive effect on EB (Fig. 3c), while chitosan had a negative effect (Fig. 2 a, b). The TS and EB values of the CAG composite films were almost similar (Figs. 2 and 3). The EB values of artificial skin prepared from a chitosan and gelatin composite were slightly higher than those of the CAG composite film. This proves that agar has a lower EB value than gelatin;⁹² a comparable result was noted in materials based on chitosan and copolymer (lactide-titanium oxide).²²

Puncture resistance (PR)

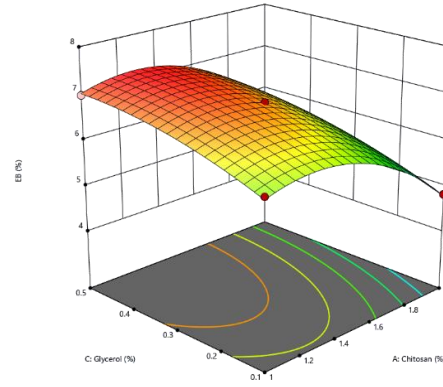
Puncture resistance of a packaging material is defined as the maximum force (N) required to penetrate it. This type of biaxial stress is normally exerted in films during packing of processed foods. The PR of a film is attributed to the microstructure of the film network and the intermolecular force.⁹³ The estimated PR values of the CAG composite films ranged from 11.74 ± 2.55 to 17.67 ± 1.64 N. The PR of the CAG films was comparable with those of carp collagen-chitosan-lemon essential oil composite films.⁹³ PR is one of the preferable mechanical properties of food packaging materials to ensure a protective packaging of irregular shape foods. The data collected from RSM based on Box-Behnken for the measurement of variables are shown in Table 2. The analysis of experimental data suits the quadratic mathematical model implied in the data and, it gave the following relationship between independent variables: $PR = + 14.32 + 1.58 A + 0.6800 B + 1.26 C - 0.8925 AB - 0.5050 AC - 0.4575 BC + 0.5215 A^2 + 0.7840 B^2 + 0.3665 C^2$. The ANOVA implied that the model was significant (Table 4), where the proposed equation matched 96.49%. The Predicted R^2 of 0.9184 is in reasonable agreement with the Adjusted R^2 of 0.9883; as the difference is less than 0.2. The Lack of Fit F-value of 1121.79 implies the Lack of Fit is significant as per the experimental values. Therefore, the chance of a lack of fit is only 0.01%. The model revealed that all independent variables showed a positive correlation with PR (Fig. 4 a, b, c). The influence of chitosan on PR was comparatively higher than that of agar. The effect of chitosan and agar on the PR value (Fig. 4a) was higher than that of chitosan and glycerol (Fig. 4b), followed by agar and glycerol (Fig. 4c). The overall PR value was highly influenced by chitosan, followed by agar and glycerol. It reveals that the bond network formed between the functional groups of chitosan and agar is comparatively stronger than in the case of glycerol.

Variable optimization and model validation

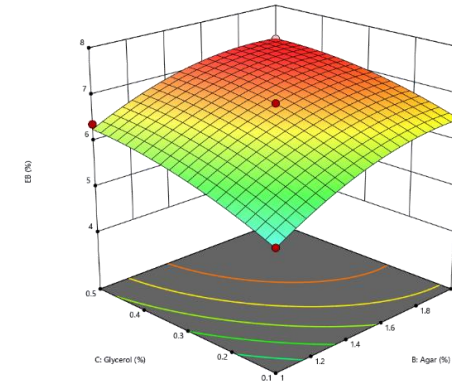
The experimental results obtained for WVP, TS, EB and PR affirmed that the evaluated independent variables were mutually responsible. The optimization of the three variables that influence the mechanical properties of the film needs more analytical skills. Hence, the optimization was performed using the desirability function and the model was calculated by Design-Expert® software to target the minimum WVP and the maximum TS, EB and PR values. The desirability function was analyzed for three independent variables (Fig. 5 a, b, c) with overlay plots (Fig. 6 a, b, c). The optimal desirable composition of the CAG film was determined to be: chitosan 1.51% (w/v), agar 2.00% (w/v) and glycerol 0.42% (w/v), whereby the overall desirability was 0.862. The validated results were found to have an absolute residual error between 1.24 and 3.56% (Table 5) for the experimental and predicted values of the optimized CAG composite film.



(a)

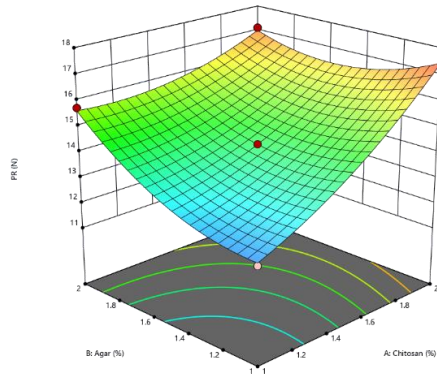


(b)

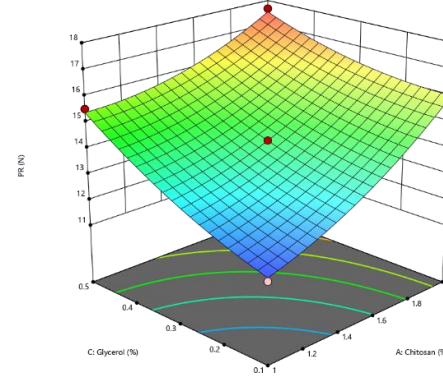


(c)

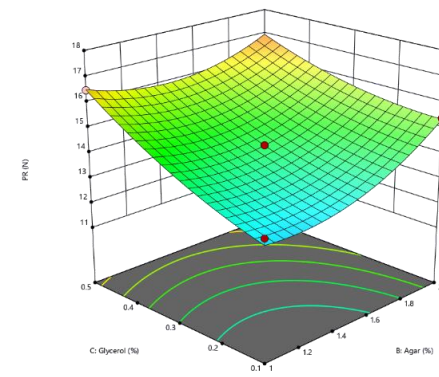
Figure 3: Response surface graphs: (a) Effect of chitosan and agar on Elongation at Break, (b) Effect of chitosan and glycerol on elongation at break, (c) Effect of agar and glycerol on elongation at break



(a)



(b)



(c)

Figure 4: Response surface graphs: (a) Effect of chitosan and agar on puncture resistance, (b) Effect of chitosan and glycerol on puncture resistance, (c) Effect of agar and glycerol on puncture resistance

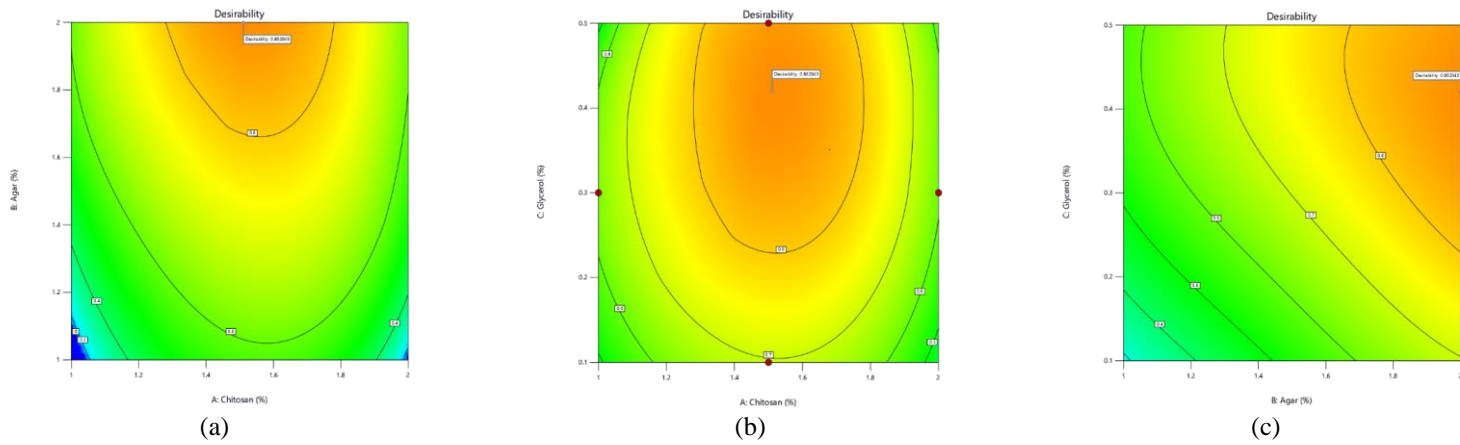


Figure 5: Desirability plots of independent variables: (a) of chitosan and agar, (b) of chitosan and glycerol, (c) of agar and glycerol

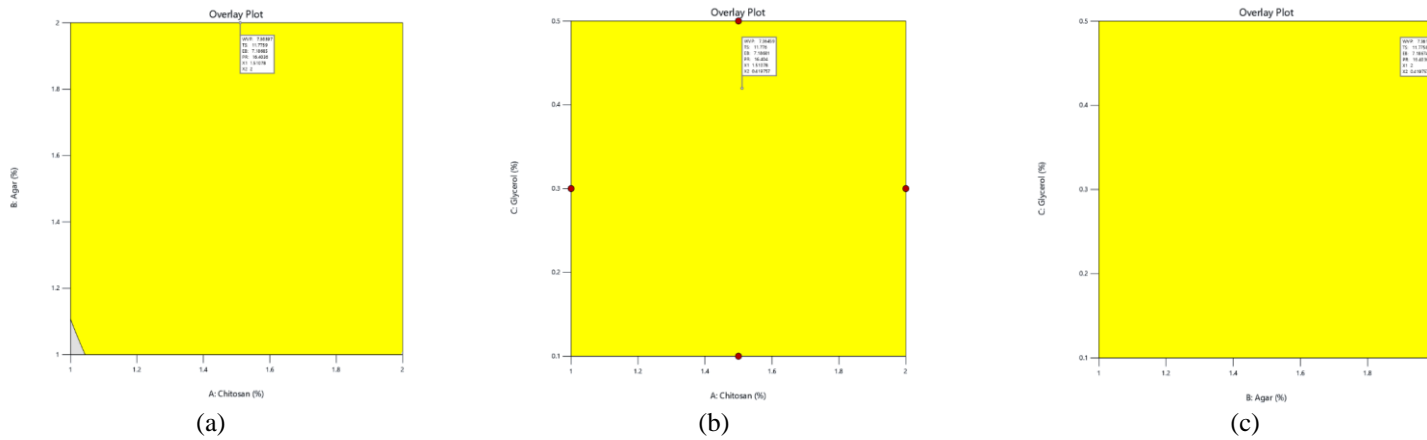


Figure 6: Overlay plots of independent variables: (a) of chitosan and agar, (b) of chitosan and glycerol, (c) of agar and glycerol

Table 5
Predicted and observed responses of optimized CAG film

Response	Predicted value ¹	Experimental value (n=3) ²	Absolute residual error (%) ³
WVP	7.16	7.25±0.04 ^a	1.24
TS	11.78	12.21±0.2 ^b	3.56
EB	7.19	7.32±0.07 ^a	1.82
PR	16.4	16.18±0.13 ^c	1.39

¹ Predicted values obtained from the model equations, ² Proportion of chitosan, agar and glycerol (1.51: 2.0: 0.42) in the optimized film, ³ Absolute residual error (%) = [(experimental value – predicted value) / experimental value] × 100.

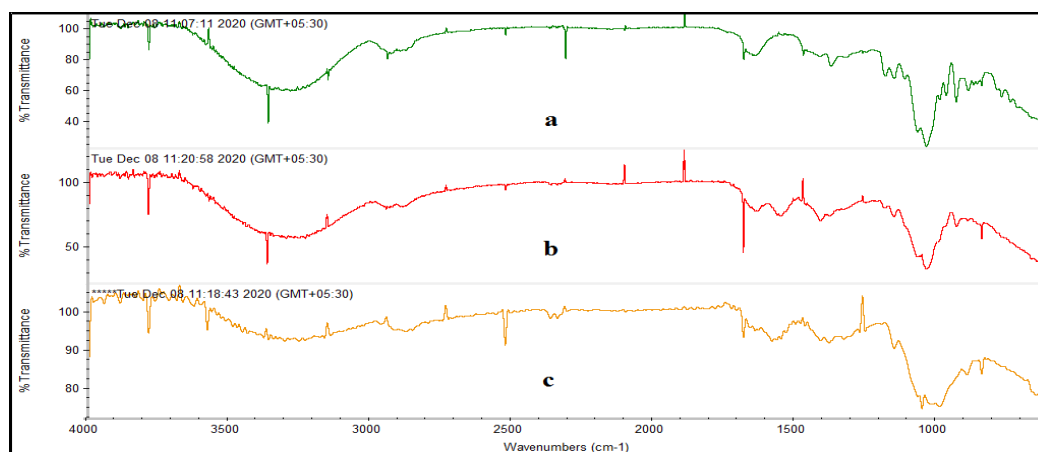


Figure 7: ATR FT-IR spectra for the films (a) with chitosan and glycerol, (b) with agar and glycerol, and (c) optimized CAG composite film

Attenuated total reflection - Fourier transform infrared spectroscopy (ATR-FTIR)

ATR-FTIR analyses were carried out to evaluate possible chemical interactions and structural changes in the functional groups among chitosan, agar and glycerol during film formation. The peaks of transmittance at different wavenumbers of the optimized CAG composite film were compared with two individual films to examine variations in interaction among the different components (Fig. 7 a, b, c). The film developed by chitosan and glycerol has a typical spectrum, as shown in Figure 7a. The broad band from 3100 cm⁻¹ to 3400 cm⁻¹ is due to the OH stretching. The peak at 1650 cm⁻¹ is attributed to C=O stretching (amide I). The band at 1500 cm⁻¹ is assigned to NH bending (amide II) (NH₂), while the bands at 2927, 2884, 1411, 1321 and 1260 cm⁻¹ are assigned to CH₂ bending due to the pyranose ring.⁹⁴ The band flapping at 1380 cm⁻¹ is due to CH₃. The chitosan spectrum characteristics of the present study are similar to those from previous reports.^{95,96}

The ATR-FTIR spectrum of the agar and glycerol film (Fig. 7b) showed the absorption band at about 3400 cm⁻¹, associated with O-H stretching,⁹⁷ and the peak at 2900 cm⁻¹, due to CH₃, CH₂ groups.⁹⁶ The bands at 1070 and 930 cm⁻¹ are associated with the 3,6-anhydro-galactose bridges.⁹⁸ The typical peak band at around 1643 cm⁻¹ is due to the stretching vibration of the conjugated peptide bond formed by amine (NH) and acetone (CO) groups.⁹⁹

The ATR-FTIR spectrum of the optimized CAG composite film (Fig. 7c) revealed the disappearance of the sharp peak corresponding to OH stretching from the individual chitosan and agar films (3350 cm⁻¹) and a noticeable reduction in deepness of the broad band in the region from 3100 cm⁻¹ to 3400 cm⁻¹. It indicates changes in the hydrogen bonding among chitosan, agar and glycerol. The CAG composite has a modified CH₂ stretching pattern from 2800 to 2900 cm⁻¹. The disappearance of CH₂ stretching located at 2350 cm⁻¹ in the spectrum of the pure agar film and the appearance of a similar new peak at 2550 cm⁻¹ in the CAG film proves a shifting bonding pattern. The noticeably higher intensity of the peak from the agar film and amide I of the chitosan altered the stretching vibration peak in the CAG composite in the region from around 1450 cm⁻¹ to 1650 cm⁻¹. The blending of chitosan with agar caused a decrease in the intensity of the band arising from NH bending (amide II) at 1560 cm⁻¹ of agar and reflected in the CAG composite film. Similarly, the CAG film revealed a decrease in the absorbance band at 1400 cm⁻¹ and an increase in the band absorbance at

1350 cm^{-1} . Furthermore, the spectra of the CAG composite film show a broadening intensive peak at 1000 cm^{-1} . The peak at 1300 cm^{-1} may be ascribed to the polysaccharide (1–4) glycosidic bond stretching vibration.¹⁰² These findings can be explained by the fact that mixing two or more polymers leads to changes in the occurrence of characteristic peaks as a reflection of the physical and chemical interactions between them.^{100,101} These observations indicate good miscibility between chitosan and agar in the presence of glycerol, which is most likely caused by the formation of intermolecular hydrogen bonds among the amino and hydroxyl groups in chitosan with the hydroxyl groups in agar.

Atomic force microscopy (AFM) analysis

The AFM analysis is an ideal technique for nano-level characterization of packaging films. It provides 3D visualization, along with qualitative and quantitative morphology insights, on many physico-chemical properties, such as size, surface smoothness and cross-sectional structure. The AFM analysis of the morphology of the optimized film provides useful information about the film substrate and reveals better understanding on properties such as MC, WVP, TS, EB, PR, WI and transparency. Moreover, it is convenient to observe the homogeneity of the composite, material orientation, material dispersion in the matrix and the presence of clumps. The surface and cross-section images of the optimized CAG composite film visualized at 1.3 μm , 630 nm and 310 nm are shown in Figure 8. 3D atomic force microscopy image of the composite film at 310 nm magnification exhibited the layer-by-layer pattern of the film structure at the nano-level. A slightly non-linear wave surface molecular interaction could be visualized at 1.3 μm .

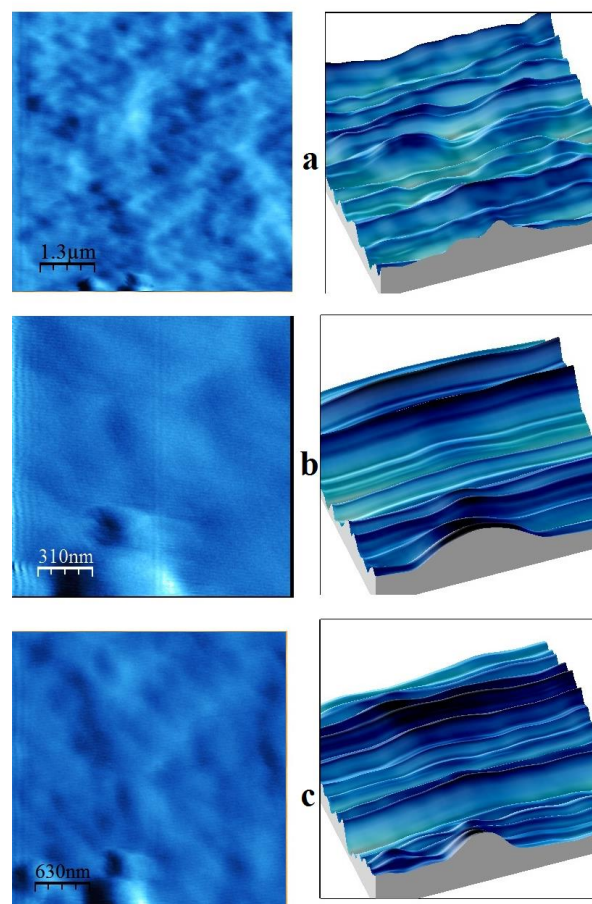


Figure 8: Atomic force microscopy images of optimized CAG composite film at: (a) 1.3 μm , (b) 310 nm, (c) 630 nm

The optimized CAG composite film was found to have good mechanical properties and thus, more functional application. The film transparency values in this study corroborate with AFM images. The regular topographical pattern seen in the images explains that the compact structure of the CAG composite film is due to the proper arrangement of the internal network, which might be responsible for its better physico-chemical, mechanical and optical properties.

CONCLUSION

The BBD-RSM has been successfully applied to develop a CAG composite film. The CAG optimized composite film demonstrated desired properties. The overall desirability function fits the quadratic model (0.862) at a significant ($p < 0.05$) level for the optimized concentration of independent variables (chitosan 1.51% (w/v), agar 2.00% (w/v) and glycerol 0.42% (w/v)) to get the minimum water vapor permeability and the maximum tensile strength, elongation at break and puncture resistance. The optimized values were validated with experimental values. The results revealed that the level of chitosan has positively contributed to the properties required for packaging materials, such as MC, swelling, erosion, WVP and PR. Likewise, agar has been found to be a responsible factor for thickness, WI, transparency, TS and EB of the optimized CAG composite film. ATR-FTIR evidenced the additional bonding responsible for higher network interaction in the film. AFM results also indicated nano-level smoothness due to the layer-by-layer arrangement of the polymers in the film, suggesting good functional properties. Therefore, the CAG composite film developed in this study can be utilized as a biodegradable packaging material in the food industry. The qualities of the CAG composite film, as revealed in the present work, recommend it as a potential packaging material with satisfactory physico-chemical, mechanical and optical properties.

ACKNOWLEDGMENT: The authors express their sincere thanks to Dr. B. Sundaramoorthi, Dean, Fisheries College and Research Institute, Thoothukudi, Tamil Nadu, India, for facilitating the study in college laboratories, and to Dr. C.N. Ravishankar, ICAR-CIFT, Cochin, India, for having provided support for analysis of optical parameters. The authors also extend their gratitude to Dr. R. Jeya Shakila, TNJFU Referral Laboratory of Fish Quality Monitoring and Certification, Tamil Nadu Dr. J. Jayalalithaa Fisheries University, Thoothukudi, Tamil Nadu, India, for the support provided for analysis of mechanical parameters, as well as to Dr. C. Vedhi, Department of Chemistry, VOC College, Thoothukudi, Tamil Nadu, India, for providing facilities for ATR-FTIR and AFM analyses.

REFERENCES

- ¹ D. Xu, T. Chen and Y. Liu, *Polym. Bull.*, **78**, 3607 (2020), <https://doi.org/10.1007/s00289-020-03294-1>
- ² L. J. Pérez-Córdoba, I. T. Norton and H. K. Batchelor, *Food Hydrocoll.*, **79**, 544 (2018), <https://doi.org/10.1016/j.foodhyd.2017.12.012>
- ³ Global plastic production 1950-2018, *Statista*, <https://www.statista.com/statistics/282732/global-production-of-plastics-since-1950/>
- ⁴ L. Lebreton and A. Andrady, *Palgrave Commun.*, **5**, 1 (2019), <https://doi.org/10.1057/s41599-018-0212-7>
- ⁵ E. Kabir, R. Kaur, J. Lee, K. H. Kim and E. E. Kwon, *J. Clean. Prod.*, **258**, 120536 (2020), <https://doi.org/10.1016/j.jclepro.2020.120536>
- ⁶ A. K. Mohanty, M. Misra and G. Hinrichsen, *Macromol. Mater. Eng.*, **276**, 1 (2000), [https://doi.org/10.1002/\(SICI\)1439-2054\(20000301\)276:1<1::AID-MAME1>3.0.CO;2-W](https://doi.org/10.1002/(SICI)1439-2054(20000301)276:1<1::AID-MAME1>3.0.CO;2-W)
- ⁷ O. V. López, N. E. Zaritzky and M. A. García, *J. Food Eng.*, **100**, 160 (2010), <https://doi.org/10.1016/j.jfoodeng.2010.03.041>
- ⁸ T. Woggum, P. Sirivongpaisal and T. Wittaya, *Int. J. Biol. Macromol.*, **67**, 490 (2014), <https://doi.org/10.1016/j.ijbiomac.2014.03.029>
- ⁹ R. C. do Lago, A. L. M. de Oliveira, M. Cordasso Dias, E. E. N. de Carvalho, G. H. Denzin Tonoli and E. V. de Barros Vilas Boas, *Ind. Crop. Prod.*, **148**, 112264 (2020), <https://doi.org/10.1016/j.indcrop.2020.112264>
- ¹⁰ S. Li, Y. Ma, T. Ji, D. E. Sameen, S. Ahmed *et al.*, *Carbohydr. Polym.*, **248**, 116805 (2020), <https://doi.org/10.1016/j.carbpol.2020.116805>
- ¹¹ S. Mali, M. V. E. Grossmann, M. A. Garcia, M. N. Martino and N. E. Zaritzky, *Carbohydr. Polym.*, **50**, 379 (2002), [https://doi.org/10.1016/S0144-8617\(02\)00058-9](https://doi.org/10.1016/S0144-8617(02)00058-9)
- ¹² E. da R. Zavareze, V. Z. Pinto, B. Klein, S. L. M. El Halal, M. C. Elias *et al.*, *Food Chem.*, **132**, 344 (2012), <https://doi.org/10.1016/j.foodchem.2011.10.090>
- ¹³ Z. Zareie, T. Yazdi and F. Mortazavi, *Carbohydr. Polym.*, **244**, 116491 (2020), <https://doi.org/10.1016/j.carbpol.2020.116491>

- ¹⁴ H. Doh, K. D. Dunno and W. S. Whiteside, *Food Biosci.*, **38**, 100795 (2020), <https://doi.org/10.1016/j.fbio.2020.100795>
- ¹⁵ S. A. A. Mohamed, M. El-Sakhawy and M. A.-M. El-Sakhawy, *Carbohydr. Polym.*, **238**, 116178 (2020), <https://doi.org/10.1016/j.carbpol.2020.116178>
- ¹⁶ J. Park, J. Nam, H. Yun, H.-J. Jin and H.W. Kwak, *Carbohydr. Polym.*, **254**, 117317 (2021), <https://doi.org/10.1016/j.carbpol.2020.117317>
- ¹⁷ P. Manivasagan and J. Oh, *Int. J. Biol. Macromol.*, **82**, 315 (2016), <https://doi.org/10.1016/j.ijbiomac.2015.10.081>
- ¹⁸ R. Jayakumar, N. Nwe, S. Tokura and H. Tamura, *Int. J. Biol. Macromol.*, **40**, 175 (2007), <https://doi.org/10.1016/j.ijbiomac.2006.06.021>
- ¹⁹ X. Jiang and X. Zhang, *Polym. Bull.*, **74**, 1817 (2017), <https://doi.org/10.1007/s00289-016-1806-0>
- ²⁰ P. C. Srinivasa, M. N. Ramesh and R. N. Tharanathan, *Food Hydrocoll.*, **21**, 113 (2007), <https://doi.org/10.1016/j.foodhyd.2006.08.005>
- ²¹ H. Wang, J. Qian and F. Ding, *J. Agric. Food. Chem.*, **66**, 395 (2018), <https://doi.org/10.1021/acs.jafc.7b04528>
- ²² E. V. Salomatina, I. R. Lednev, N. E. Silina, E. A. Gracheva, A. S. Koryagin *et al.*, *Polym. Bull.*, **77**, 5083 (2020), <https://doi.org/10.1007/s00289-019-03007-3>
- ²³ P. J. A. Sobral, F. C. Menegalli, M. D. Hubinger and M. A. Roques, *Food Hydrocoll.*, **15**, 423 (2001), [https://doi.org/10.1016/S0268-005X\(01\)00061-3](https://doi.org/10.1016/S0268-005X(01)00061-3)
- ²⁴ M. Martínez-Sanz, L. G. Gómez-Mascaraque, A. R. Ballester, A. Martínez-Abad, A. Brodkorb *et al.*, *Algal Res.*, **38**, 101420 (2019), <https://doi.org/10.1016/j.algal.2019.101420>.
- ²⁵ R. Armisen and F. Gaiatas, in “Handbook of Hydrocolloids”, edited by G. O. Phillips, P. A. Williams, 2nd ed., Woodhead Publishing, 2009, p. 82-107, <https://doi.org/10.1533/9781845695873.82>
- ²⁶ T. R. Laaman (Ed.), “Hydrocolloids in Food Processing”, Oxford, UK, Wiley-Blackwell, 2011
- ²⁷ M. B. Nieto and M. Akins, “Hydrocolloids in Food Processing”, Blackwell Publishing, 2010, pp. 67-107
- ²⁸ R. Armisen and F. Gaiatas, in “Handbook of Hydrocolloids”, edited by G. O. Phillips, P. A. Williams, 2nd ed., Woodhead Publishing, 2009, p. 82-107, <https://doi.org/10.1533/9781845695873.82>
- ²⁹ F. S. Mostafavi and D. Zaeim, *Int. J. Biol. Macromol.*, **159**, 1165 (2020), <https://doi.org/10.1016/j.ijbiomac.2020.05.123>
- ³⁰ S. Alvarado, G. Sandoval, I. Palos, S. Tellez, Y. Aguirre-Loredo *et al.*, *Food Sci. Technol.*, **35**, 690 (2015), <https://doi.org/10.1590/1678-457X.6797>
- ³¹ A. Awadhiya, D. Kumar, K. Rathore, F. Bushara and V. Vivek, *Polym. Bull.*, **74**, 2887 (2017), <https://doi.org/10.1007/s00289-016-1872-3>
- ³² W. N. Syahirah, N. A. Azami, K. H. Huong and A. A. Amirul, *Polym. Bull.*, **78**, 3973 (2020), <https://doi.org/10.1007/s00289-020-03286-1>
- ³³ J. Vallejo-Montesinos, J. Gámez-Cordero, R. Zarraga, M. C. P. Pérez and J. A. Gonzalez-Calderon, *Polym. Bull.*, **77**, 107 (2020), <https://doi.org/10.1007/s00289-019-02740-z>
- ³⁴ S. Gopi, A. Pius, R. Kargl, K. S. Kleinschek and S. Thomas, *Polym. Bull.*, **76**, 1557 (2019), <https://doi.org/10.1007/s00289-018-2467-y>
- ³⁵ S. H. Kim, B. K. Lim, F. Sun, K. Koh, S. C. Ryu *et al.*, *Polym. Bull.*, **62**, 111 (2009), <https://doi.org/10.1007/s00289-008-1008-5>
- ³⁶ M. Aslam, Z. A. Raza and A. Siddique, *Polym. Bull.*, **78**, 1955 (2020), <https://doi.org/10.1007/s00289-020-03194-4>
- ³⁷ V. Venugopal, *ECronicon. Nutr.*, **14**, 126 (2019)
- ³⁸ L. E. Rioux, S. L. Turgeon and M. Beaulieu, *J. Sci. Food Agric.*, **87**, 1630 (2007), <https://doi.org/10.1002/jsfa.2829>
- ³⁹ V. Venugopal, in “Marine Polysaccharides: Food Applications”, CRC Press, Boca Raton, FL, USA, 2011, pp. 111-122
- ⁴⁰ D. L. Arvizu-Higuera, Y. E. Rodríguez-Montesinos, J. I. Murillo-Álvarez, M. Muñoz-Ochoa and G. Hernández-Carmona, in *Procs. Nineteenth International Seaweed Symposium*, Springer, Dordrecht, 2007, pp. 65-69
- ⁴¹ V. Siracusa, P. Rocculi, S. Romani and M. D. Rosa, *Trends Food Sci. Technol.*, **19**, 634 (2008), <https://doi.org/10.1016/j.tifs.2008.07.003>
- ⁴² N. Chopin, X. Guillory, P. Weiss, J. L. Bideau and S. Colliet-Jouault, *Curr. Org. Chem.*, **18**, 867 (2014), <https://doi.org/10.2174/138527281807140515152334>
- ⁴³ F. Debeaufort, J. A. Quezada-Gallo and A. Voilley, *Crit. Rev. Food Sci. Nutr.*, **38**, 299 (1998), <https://doi.org/10.1080/10408699891274219>
- ⁴⁴ G. Kerch and V. Korkhov, *Eur. Food Res. Technol.*, **232**, 17 (2011), <https://doi.org/10.1007/s00217-010-1356-x>

- ⁴⁵ M. S. Lee, S. H. Lee, Y. H. Ma, S. K. Park, D. H. Bae *et al.*, *Prev. Nutr. Food Sci.*, **2005**, 88 (2005), <https://doi.org/10.3746/jfn.2005.10.1.088>
- ⁴⁶ J. H. Han and G. Aristippos, in “Innovations in Food Packaging”, edited by J. H. Han, Academic Press, London, 2005, pp. 239-262, <https://doi.org/10.1016/B978-012311632-1/50047-4>
- ⁴⁷ J. P. Maran, V. Sivakumar, R. Sridhar and K. Thirugnanasambandham, *Carbohydr. Polym.*, **92**, 1335 (2013), <https://doi.org/10.1016/j.carbpol.2012.09.069>
- ⁴⁸ A. M. Youssef, M. Samah and E. L. Sayed, *Carbohydr. Polym.*, **193**, 19 (2018), <https://doi.org/10.1016/j.carbpol.2018.03.088>
- ⁴⁹ A. Nešić, G. Cabrera-Barjas, S. Dimitrijević-Branković, S. Davidović, N. Radovanović *et al.*, *Molecules*, **25**, 135 (2020), <https://doi.org/10.3390/molecules25010135>
- ⁵⁰ N. S. Said and N. M. Sarbon, *Polym. Testing*, **81**, 106161 (2020), <https://doi.org/10.1016/j.polymertesting.2019.106161>
- ⁵¹ K. Kaur and R. Jindal, *Polym. Bull.*, **76**, 3569 (2019), <https://doi.org/10.1007/s00289-018-2555-z>
- ⁵² M. Rangel-Marrón, E. Mani-López, E. Palou and A. López-Malo, *LWT*, **101**, 83 (2019), <https://doi.org/10.1016/j.lwt.2018.11.005>
- ⁵³ N. Blanco-Pascual, M. P. Montero and M. C. Gómez-Guillén, *Food Hydrocoll.*, **37**, 100 (2014), <https://doi.org/10.1016/j.foodhyd.2013.10.021>
- ⁵⁴ M. Bajić, H. Jalšovec, A. Travan, U. Novak and B. Likozar, *Carbohydr. Polym.*, **219**, 261 (2019), <https://doi.org/10.1016/j.carbpol.2019.05.003>
- ⁵⁵ H. Doh, K. D. Dunno and W. S. Whiteside, *Food Hydrocoll.*, **105**, 105744 (2020), <https://doi.org/10.1016/j.foodhyd.2020.105744>
- ⁵⁶ A. Farhan and N. M. Hani, *Food Packag. Shelf Life*, **24**, 100476 (2020), <https://doi.org/10.1016/j.fpsl.2020.100476>
- ⁵⁷ J. H. Han and J. D. Floros, *J. Plast. Film Sheet.*, **13**, 287 (1997), <https://doi.org/10.1177/875608799701300405>
- ⁵⁸ J. G. Meher, M. Tarai, N. P. Yadav, A. Patnaik, P. Mishra *et al.*, *Carbohydr. Polym.*, **96**, 172 (2013), <https://doi.org/10.1016/j.carbpol.2013.03.076>
- ⁵⁹ ASTM, Standard Designations E96/E96M, Annual Book of ASTM Standards, American Society for Testing and Materials, Philadelphia, PA, 2016
- ⁶⁰ ASTM, American Society for Testing and Materials, 1995
- ⁶¹ K. Iwata, S. Ishizaki, A. Handa and M. Tanaka, *Fish. Sci.*, **66**, 372 (2000), <https://doi.org/10.1046/j.1444-2906.2000.00057.x>
- ⁶² M. Ahmad and S. Benjakul, *Food Hydrocoll.*, **25**, 381 (2011), <https://doi.org/10.1016/j.foodhyd.2010.07.004>
- ⁶³ L. Van der Meeren, J. Verduijn, D. V. Krysko and A. G. Skirtach, *IScience*, **23**, 101816 (2020), <https://doi.org/10.1016/j.isci.2020.101816>
- ⁶⁴ R. Y. Aguirre-Loredo, A. I. Rodríguez-Hernández, E. Morales-Sánchez, C. A. Gómez-Aldapa and G. Velazquez, *Food Chem.*, **196**, 560 (2016), <https://doi.org/10.1016/j.foodchem.2015.09.065>
- ⁶⁵ P. M. Rahman, V. A. Mujeeb and K. Muraleedharan, *Polym. Bull.*, **74**, 3399 (2017), <https://doi.org/10.1007/s00289-016-1901-2>
- ⁶⁶ M. T. Soe, T. Pongjanyakul, E. Limpongsa and N. Jaipakdee, *Carbohydr. Polym.*, **245**, 116556 (2020), <https://doi.org/10.1016/j.carbpol.2020.116556>
- ⁶⁷ R. Ahmadi, A. Kalbasi-Ashtari, A. Oromiehie, M. S. Yarmand and F. Jahandideh, *J. Food Eng.*, **109**, 745 (2012), <https://doi.org/10.1016/j.jfoodeng.2011.11.010>
- ⁶⁸ X. Ma, C. Qiao, X. Wang, J. Yao and J. Xu, *Int. J. Biol. Macromol.*, **135**, 240 (2019), <https://doi.org/10.1016/j.ijbiomac.2019.05.158>
- ⁶⁹ N. Nordin, S. H. Othman, S. A. Rashid and R. K. Basha, *Food Hydrocoll.*, **106**, 105884 (2020), <https://doi.org/10.1016/j.foodhyd.2020.105884>
- ⁷⁰ S. Galus and A. Lenart, *J. Food Eng.*, **115**, 459 (2013), <https://doi.org/10.1016/j.jfoodeng.2012.03.006>
- ⁷¹ M. A. García, A. Pinotti, M. N. Martino and N. E. Zaritzky, in “Edible Films and Coatings for Food Applications”, edited by K. Huber, M. Embuscado, Springer, New York, 2009, pp. 169-209, https://link.springer.com/chapter/10.1007/978-0-387-92824-1_6
- ⁷² H. Sudaryati, S. T. Mulyani and E. R. Hansyah, *Jurnal Teknologi Pertanian*, **11**, 196 (2012)
- ⁷³ R. Thakur, B. Saberi, P. Pristijono, C. E. Stathopoulos, J. B. Golding *et al.*, *J. Food Sci. Technol.*, **54**, 2270 (2017), <https://doi.org/10.1007/s13197-017-2664-y>
- ⁷⁴ Z. Mahcene, A. Khelil, S. Hasni, P. K. Akman, F. Bozkurt *et al.*, *Int. J. Biol. Macromol.*, **145**, 124 (2020), <https://doi.org/10.1016/j.ijbiomac.2019.12.093>
- ⁷⁵ M. Nagarajan, S. Benjakul, T. Prodpran and P. Songtipya, *J. Food Sci. Technol.*, **52**, 7669 (2015), <https://doi.org/10.1007/s13197-015-1905-1>
- ⁷⁶ D. Liu and L. Zhang, *Macromol. Mater. Eng.*, **291**, 820 (2006), <https://doi.org/10.1002/mame.200600098>

- ⁷⁷ H. T. Kevij, M. Salami, M. Mohammadian, M. Khodadadi and Z. K. Emam-Djomeh, *Polym. Bull.*, **78**, 4387 (2020), <https://doi.org/10.1007/s00289-020-03319-9>
- ⁷⁸ B. H. Chen, W. S. Kuo and L. S. Lai, *Food Hydrocoll.*, **24**, 200 (2010), <https://doi.org/10.1016/j.foodhyd.2009.09.006>
- ⁷⁹ A. Saaraï, T. Sedlacek, V. Kasparkova, T. Kitano and P. Saha, *J. Appl. Polym. Sci.*, **126**, E79 (2012), <https://doi.org/10.1002/app.36590>
- ⁸⁰ A. Chetouani, M. Elkolli, M. Bounekhel and D. Benachour, *Polym. Bull.*, **74**, 4297 (2017), <https://doi.org/10.1007/s00289-017-1953-y>
- ⁸¹ N. A. Nafee, F. A. Ismail, N. A. Boraie and L. M. Mortada, *Drug Dev. Ind. Pharm.*, **30**, 985 (2004), <https://doi.org/10.1081/DDC-200037245>
- ⁸² M. Shaikh, S. Haider, T. M. Ali and A. Hasnain, *Int. J. Biol. Macromol.*, **124**, 209 (2019), <https://doi.org/10.1016/j.ijbiomac.2018.11.135>
- ⁸³ K. S. Sandhu, L. Sharma, M. Kaur and R. Kaur, *Int. J. Biol. Macromol.*, **143**, 704 (2020), <https://doi.org/10.1016/j.ijbiomac.2019.09.111>
- ⁸⁴ A. de Lima Barizão, M. I. Crepaldi, O. de O. S. Junior, A. C. de Oliveira, A. F. Martins *et al.*, *Int. J. Biol. Macromol.*, **165**, 582 (2020), <https://doi.org/10.1016/j.ijbiomac.2020.09.150>
- ⁸⁵ N. Singh, P. S. Belton and D. M. R. Georget, *Int. J. Biol. Macromol.*, **45**, 116 (2009), <https://doi.org/10.1016/j.ijbiomac.2009.04.006>
- ⁸⁶ S. Saedi, M. Shokri and J. W. Rhim, *Food Hydrocoll.*, **106**, 105934 (2020), <https://doi.org/10.1016/j.foodhyd.2020.105934>
- ⁸⁷ I. K. Sani, S. Pirsá and S. Tađı, *Polym. Test.*, **79**, 106004 (2019), <https://doi.org/10.1016/j.polymertesting.2019.106004>
- ⁸⁸ P. C. Srinivasa, R. Ravi and R. N. Tharanathan, *J. Food Eng.*, **80**, 184 (2007), <https://doi.org/10.1016/j.jfoodeng.2006.05.007>
- ⁸⁹ R. Arham, M. T. Mulyati, M. Metusalach and S. Salengke, *Int. Food Res. J.*, **23**, 1669 (2016)
- ⁹⁰ S. A. Mir, B. N. Dar, A. A. Wani and M. A. Shah, *Trends Food Sci. Technol.*, **80**, 141 (2018), <https://doi.org/10.1016/j.tifs.2018.08.004>
- ⁹¹ F. Luzi, L. Torre, J. M. Kenny and D. Puglia, *Materials*, **12**, 471 (2019), <https://doi.org/10.3390/ma12030471>
- ⁹² S. Parvez, M. M. Rahman, M. A. Khan, M. A. H. Khan, J. M. Islam *et al.*, *Polym. Bull.*, **69**, 715 (2012), <https://doi.org/10.1007/s00289-012-0761-7>
- ⁹³ Y. Jiang, W. Lan, D. E. Sameen, S. Ahmed, W. Qin *et al.*, *Int. J. Biol. Macromol.*, **160**, 340 (2020), <https://doi.org/10.1016/j.ijbiomac.2020.05.202>
- ⁹⁴ A. Pawlak and M. Mucha, *Thermochim. Acta*, **396**, 153 (2003), [https://doi.org/10.1016/S0040-6031\(02\)00523-3](https://doi.org/10.1016/S0040-6031(02)00523-3)
- ⁹⁵ J. Nunthanid, S. Puttipipatkachorn, K. Yamamoto and G. E. Peck, *Drug Dev. Ind. Pharm.*, **27**, 143 (2001), <https://doi.org/10.1081/DDC-100000481>
- ⁹⁶ E. A. El-hefian, M. M. Nasef and A. H. Yahaya, *J. Chem.*, **9**, 1431 (2012), <https://doi.org/10.1155/2012/781206>
- ⁹⁷ M. Tako, M. Higa, K. Medoruma and Y. Nakasone, *Bot. Mar.*, **42**, 513 (1999), <https://doi.org/10.1515/BOT.1999.058>
- ⁹⁸ M. Sekkal and P. Legrand, *Spectrochim. Acta, Part Mol. Spectrosc.*, **49**, 209 (1993), [https://doi.org/10.1016/0584-8539\(93\)80176-B](https://doi.org/10.1016/0584-8539(93)80176-B)
- ⁹⁹ A. Christiaen and M. Bodard, *Papenfuss. Bot. Mar.*, **26**, 425 (1983), <https://doi.org/10.1515/botm.1983.26.9.425>
- ¹⁰⁰ Y. Guan, X. Liu, Y. Zhang and K. Yao, *J. Appl. Polym. Sci.*, **67**, 1965 (1998), [https://doi.org/10.1002/\(SICI\)1097-4628\(19980321\)67:12<1965::AID-APP2>3.0.CO;2-L](https://doi.org/10.1002/(SICI)1097-4628(19980321)67:12<1965::AID-APP2>3.0.CO;2-L)
- ¹⁰¹ Y. J. Yin, K. D. Yao, G. X. Cheng and J. B. Ma, *Polym. Int.*, **48**, 429 (1999), [https://doi.org/10.1002/\(SICI\)1097-0126\(199906\)48:6<429::AID-PI160>3.0.CO;2-1](https://doi.org/10.1002/(SICI)1097-0126(199906)48:6<429::AID-PI160>3.0.CO;2-1)
- ¹⁰² J. Wu, F. Zhong, Y. Li, C. F. Shoemaker and W. Xia, *Food Hydrocoll.*, **30**, 82 (2013), <https://doi.org/10.1016/j.foodhyd.2012.04.002>